Magnetic molecules created by hydrogenation of polycyclic aromatic hydrocarbons

J. A. Vergés*
Departamento de Teoría de la Materia Condensada, Instituto de Ciencia de Materiales de Madrid (CSIC), Cantoblanco, 28049 Madrid, Spain

G. Chiappe and E. Louis
Departamento de Física Aplicada, Unidad Asociada del CSIC and Instituto Universitario de Materiales, Universidad de Alicante, San Vicente del Raspeig, 03690 Alicante, Spain

L. Pastor-Abia and E. SanFabián
Departamento de Química Física, Unidad Asociada del CSIC and Instituto Universitario de Materiales, Universidad de Alicante, San Vicente del Raspeig, 03690 Alicante, Spain
(Received 30 July 2008; published 3 March 2009)

Present routes to produce magnetic organic-based materials adopt a common strategy: the use of magnetic species (atoms, polyradicals, etc.) as building blocks. We explore an alternative approach which consists of selective hydrogenation of polycyclic aromatic hydrocarbons. Self-consistent-field (SCF) (Hartree-Fock and density-functional theory) and multiconfigurational (configuration interaction with single- and double-excitation and multiconfigurational SCF) calculations on coronene and corannulene, both hexahydrogenated, show that the formation of stable high spin species is possible. The spin of the ground states is discussed in terms of Hund's rule and Lieb's theorem for bipartite lattices (alternant hydrocarbons in this case). This proposal opens a door to magnetism in the organic world.

DOI: 10.1103/PhysRevB.79.094403 PACS number(s): 31.10.+z, 31.15.aq, 33.15.Kr, 75.50.Xx

I. INTRODUCTION

Two successful routes that are being actually followed to produce magnetic organic materials[1] are the addition of magnetic atoms[2] and the use of polyradicals.[3] In particular, carbon-based nickel compounds that show spontaneous field-dependent magnetization and hysteresis at room temperature have been recently synthesized.[2] Moreover, the combination of two radical modules with different spins has allowed the obtaining of organic polymers with ferromagnetic or antiferromagnetic ordering.[4] Research on molecules containing polyradicals goes back to the early 1990s (Refs. 3 and 5–7) and has produced a variety of results as, for example, the synthesis of high spin organic molecules. In some of these molecules the failure of Hund's rule has been demonstrated.[5] On the other hand, experimental and theoretical evidence has been recently presented indicating that 5-dehydro-m-xylylene or DMX was the first example of an organic triradical with an open-shell doublet ground state.[6,7] Both methods share a common strategy: the use of ingredients (either radicals or atoms) that provide a finite spin.

In this work we follow a different approach. Specifically, we predict the existence of spin polarized organic molecules derived from nonmagnetic π-conjugated polycyclic aromatic hydrocarbons (PAHs) by selective hydrogenation of their peripheral C atoms. High hydrogenation of PAHs has been proposed as a method for hydrogen storage.[8] More recently, the feasibility of double hydrogenation of those compounds has been investigated theoretically.[9]

Our work is inspired from Lieb's theorem for bipartite lattices that shows the appearance of magnetism whenever they are unbalanced.[10] According to Lieb,[10] if a nearest-neighbor model with a local on-site interaction is applicable to a bipartite lattice, the spin multiplicity of the ground state is $|N_A - N_B| + 1$, where N_A and N_B are the number of atoms in each sublattice. Most PAHs are alternant hydrocarbons where carbon atoms can be separated into two disjoint subsets so that an atom in one set only has neighbors in the other set (Figs. 1 and 2 show a colored version of the partition). The same theorem has been used to support the existence of magnetism in graphene ribbons and islands.[11] All work we know is based on single-determinantal methods, i.e., on a more or less sophisticated form of self-consistent-field (SCF) calculation. Let us remark that being π-orbital magnetism a direct result of the strong correlation among π electrons, only methods designed explicitly to catch these effects [such as configuration interaction with single and double excitations (CISDs) and multiconfigurational self-consistent-field (MCSCF) used in our work] can help to resolve the doubts regarding the appearance of magnetism in graphite-derived systems.

The rest of the paper is organized as follows. The *ab initio* methods (both monodeterminantal and multideterminantal) used in this work are discussed in some detail in Sec. II, while the results obtained with those methods are reported and discussed in Sec. III. Section IV, in turn, is devoted to the analysis of the *ab initio* results by means of model Hamiltonians, in particular the Hubbard and the Pariser-Parr-Pople (PPP) Hamiltonians.[12,13] Finally, the conclusions of our work are gathered in Sec. V.

II. *AB INITIO* CALCULATIONS: METHODS AND NUMERICAL PROCEDURES

Calculations of the spin states of the molecules of Figs. 1 and 2 were done using the following basis functions sets: MIDI,[14] cc-pVDZ, and cc-pVTZ.[15] Although the latter set

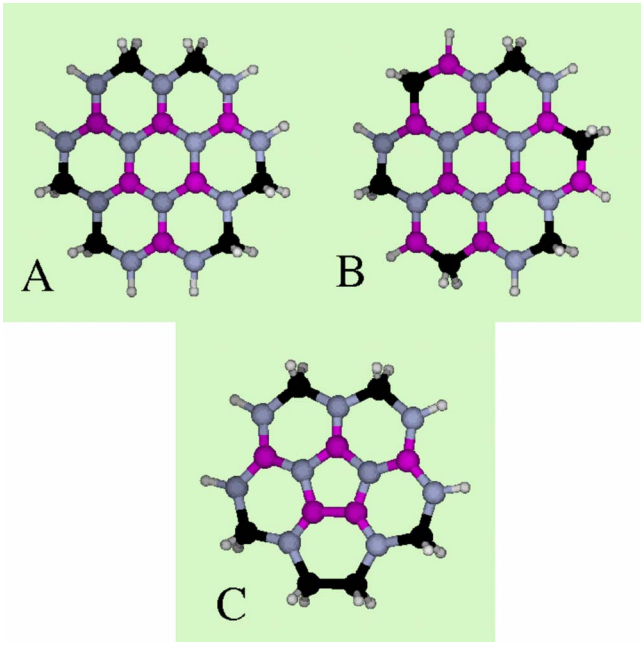

FIG. 1. (Color online) 1,4,5,8,9,12-hexahydrocoronene [(A) hereafter referred to as D_{3h} according to its symmetry group], 1,3,5,7,9,11-hexahydrocoronene [(B) hereafter referred to as C_{3h}], and planar 1,4,5,6,7,10-hexahydrocorannulene [(C) hereafter referred to as C_{2v}]. Saturated carbon atoms are represented by black symbols while dark gray (magenta) and light gray symbols are used to distinguish carbon atoms belonging to different sublattices. Corannulene is a nonalternant hydrocarbon, that is, a frustrated cluster of carbon atoms (note the fully magenta bond between two magenta atoms).

guarantees a sufficient precision, varying the dimension of the variational space allowed to check the reliability of our results. SCF calculations were carried out at the restricted-Hartree-Fock (RHF) level and by means of the hybrid density-functional RB3LYP.[16–18] In both cases the restricted-open-shell variant was used in order to get well-defined total spin values.[19] In order to check the accuracy of the description of the correlation energy of partially filled π shells, multiconfigurational wave-function calculations were also performed. CISD calculations[20] were carried out in all cases, while some checks were also made by means of the MCSCF on the fully optimized set in the active space version.[21,22] The active space was generated within the following windows $(m+n,N)$ of m occupied and n empty π molecular orbitals (MOs) filled with N electrons: hexahydrogenated coronene $S=0$ $(8+6,16)$ and $S=3$ $(11+3,16)$ and planar hexahydrogenated corannulene $S=0$ $(6+6,12)$ and $S=2$ $(8+4,12)$. Other π-MOs lie excessively far from the highest occupied molecular orbital (HOMO)–lowest unoccupied molecular orbital (LUMO) gap to give a sizable contribution. Geometries were only optimized at the SCF (RB3LYP) level.

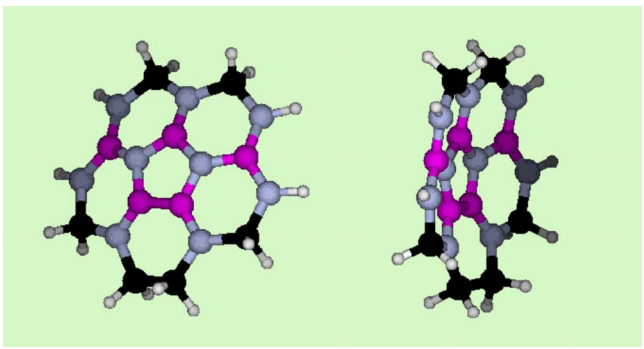

FIG. 2. (Color online) Two views of curved 1,4,5,6,7,10-hexahydrocorannulene in the calculated stable geometry (hereafter referred to as C_1). As in Fig. 1, black symbols indicate carbon atoms forming only single bonds while dark gray (magenta) and light gray symbols denote each of the two sublattices in which carbon atoms can be separated.

TABLE I. Total energies (in hartree) for atomic hydrogen, molecular hydrogen, coronene $C_{24}H_{12}$, corannulene $C_{20}H_{10}$, two molecules obtained from hexahydrogenation of coronene, and one derived from hexahydrogenation of corannulene [in the latter case the results correspond to the planar geometry shown in Fig. 1(C)]. The results were obtained using three basis sets (MIDI, cc-pVDZ, and cc-pVTZ), two SCF methods (RHF and RB3LYP), and one multiconfigurational method CISD. The number of occupied (m) and empty (n) π molecular orbitals included in the CISD calculations as well as the number of electrons that fill them (N) is indicated as $(m+n,N)$. Small stars emphasize the spin multiplicity of the more stable state.

		Basis set		
Molecule	Method	MIDI	cc-pVDZ	cc-pVTZ
H	RHF	−0.4970	−0.4993	−0.4998
	RB3LYP	−0.4953	−0.4979	−0.4988
H_2	RHF	−1.1217	−1.1287	−1.1330
	RB3LYP	−1.1623	−1.1668	−1.1733
Coronene	RHF	−910.4869	−916.0197	−916.2293
$C_{24}H_{12}$	RB3LYP	−915.9341	−921.3874	−921.6253
Corannulene	RHF	−758.6127	−763.2326	−763.4078
$C_{20}H_{10}$	RB3LYP	−763.1633	−767.7138	−767.9092
$C_{24}H_{18}$	RHF	−913.6339	−919.2239	−919.4337
$\star D_{3h}(S=3)\star$	RB3LYP	−919.1814	−924.6701	−924.9159
	CISD(11+3,16)	−913.7112	−919.2905	−919.4939
$C_{24}H_{18}$	RHF	−913.3714	−918.9826	−919.2040
$D_{3h}(S=0)$	RB3LYP	−919.0751	−924.5639	−924.8175
	CISD(8+6,16)	−913.4988	−919.0286	−919.2431
$C_{24}H_{18}$	RHF	−913.5690	−919.1638	−919.3742
$C_{3h}(S=3)$	RB3LYP	−919.1228	−924.6146	−924.8620
	CISD(11+3,16)	−913.6153	−919.2027	−919.4078
$C_{24}H_{18}$	RHF	−913.7732	−919.3607	−919.5746
$\star C_{3h}(S=0)\star$	RB3LYP	−919.3423	−924.8230	−925.0730
	CISD(8+6,16)	−913.8433	−919.4158	−919.6110
$C_{20}H_{16}$	RHF	−761.9008	−766.5625	−766.7408
$\star C_{2v}(S=2)\star$	RB3LYP	−766.5503	−771.1250	−771.3348
	CISD(8+4,12)	−761.9652	−766.6291	−766.8014
$C_{20}H_{16}$	RHF	−761.7591	−766.4418	−766.6266
$C_{2v}(S=0)$	RB3LYP	−766.4913	−771.0760	−771.2842
	CISD(6+6,12)	−761.8264	−766.4643	−766.6588

TABLE II. Fragmentation energies (in hartree) of molecules derived from hexahydrogenation of coronene and of corannulene. Total energy differences are given both for atomic and molecular forms of hydrogen. Data of Table I have been used and again small stars emphasize the spin multiplicity of the more stable state.

		Atomic H		Molecular H_2	
Molecule	Method	MIDI	cc-pVTZ	MIDI	cc-pVTZ
$C_{24}H_{18}$	RHF	−0.1651	−0.2056	0.2181	0.1946
$\star D_{3h}(S=3)\star$	RB3LYP	−0.2755	−0.2980	0.2396	0.2292
$C_{24}H_{18}$	RHF	0.0974	0.0242	0.4805	0.4243
$D_{3h}(S=0)$	RB3LYP	−0.1692	−0.1996	0.3459	0.3276
$C_{24}H_{18}$	RHF	−0.1002	−0.1460	0.2830	0.2542
$C_{3h}(S=3)$	RB3LYP	−0.2170	−0.2441	0.2982	0.2831
$C_{24}H_{18}$	RHF	−0.3044	−0.3465	0.0788	0.0537
$\star C_{3h}(S=0)\star$	RB3LYP	−0.4365	−0.4551	0.0787	0.0720
$C_{20}H_{16}$	RHF	−0.3061	−0.3342	0.0770	0.0660
$\star C_{2v}(S=2)\star$	RB3LYP	−0.4152	−0.4290	0.0999	0.0981
$C_{20}H_{16}$	RHF	−0.1644	−0.2200	0.2187	0.1802
$C_{2v}(S=0)$	RB3LYP	−0.3562	−0.3784	0.1589	0.1487
$C_{20}H_{16}$	RHF	−0.3024	−0.3259	0.0807	0.0743
$\star C_1(S=2)\star$	RB3LYP	−0.4098	−0.4198	0.1054	0.1073
$C_{20}H_{16}$	RHF	−0.1607	−0.2072	0.2224	0.1930
$C_1(S=0)$	RB3LYP	−0.3471	−0.3643	0.1680	0.1628

The geometry of 6*H*-corannulene was optimized for both its planar metastable form and its curved stable form (see Figs. 1(C) and 2). However, in order to allow a discussion in terms of π-orbital models, the results for the energies of its spin states discussed hereafter correspond to the planar geometry. Anyhow, energy differences between the spin states of the two allotropes are very small (fragmentation energies for both planar and curved geometries are reported below). All quantum chemistry calculations were done using the GAMESS program.[23]

III. *AB INITIO* CALCULATIONS: RESULTS

Total energies for the singlet and the relevant multiplet of hydrogenated coronene D_{3h}, C_{3h}, and planar hydrogenated corannulene C_{2v} (A, B, and C in Fig. 1) are reported in Table I. It is first noted that whereas the energies obtained with the small basis set MIDI and those obtained with the already large cc-pVDZ differ in 4–6 hartree (approximately 0.6%), the difference is reduced to 0.1–0.3 hartree (approximately 0.02%) when cc-pVDZ is replaced by the largest basis used in this work, namely, the cc-pVTZ basis set. This indicates that convergence, as far as the basis set is concerned, is rather acceptable. In the case of hexahydrogenated coronene (briefly 6*H*-coronene), results clearly show that, no matter the method or the basis set used, the ground state of molecule D_{3h} is a septuplet and that of molecule C_{3h} is a singlet. We have checked that other spin states lie between those two. In molecule D_{3h} the largest energy difference between the high spin ground state and the singlet occurs for RHF (0.23–0.26 hartree). This difference is reduced to approximately 0.1 hartree for RB3LYP, increasing again using the CISD method. On the other hand, all results for C_{3h} conformation show that the singlet is below the septuplet by more than 0.2 hartree. Similar results are obtained for 6*H*-corannulene although energy differences are slightly smaller. Table I also reports total-energy results for atomic and molecular hydrogen, coronene, and corannulene that allow the calculation of fragmentation energies (Table II, analysis). These are negative relative to atomic hydrogen but not relative to the molecular form. Therefore, actual synthesis of the hydrogenated molecules would need sophisticated reaction paths.[24] We also note that the singlet ground state of C_{3h} hydrogenated coronene is more stable than that of the molecule having a septuplet ground state (D_{3h}). Presumably, other forms of 6*H*-corannulene would also show deeper ground-state energies than that of the studied magnetic conformation. Note also that hydrogenation of the curved (stable) geometry of corannulene (see Fig. 2) is slightly less favorable than that of its planar geometry (compare results for C_{2v} and C_1 in Table II). Anyhow, as in the planar geometry, the quintuplet has a lower energy than the singlet.

Figure 3 depicts the total spin densities of the septuplet states ($S=3$) of 1,4,5,8,9,12-hexahydrocoronene and 1,3,5,7,9,11-hexahydrocoronene (A and B) and the quintuplet ($S=2$) of planar 1,4,5,6,7,10-hexahydrocorannulene. Concerning 1,4,5,8,9,12-hexahydrocoronene, the most appealing result is that the spin density is finite only on the carbon atoms of one sublattice. More precisely, spin density is located in the sublattice to which no additional H atoms were attached. This result is highly illustrative allowing some intuition on the reasons for a magnetic ground state: electron-electron repulsion is minimized because each electron avoids sitting at nearest-neighbor distances from the others. However, in 1,3,5,7,9,11-hexahydrocoronene, a molecule with a

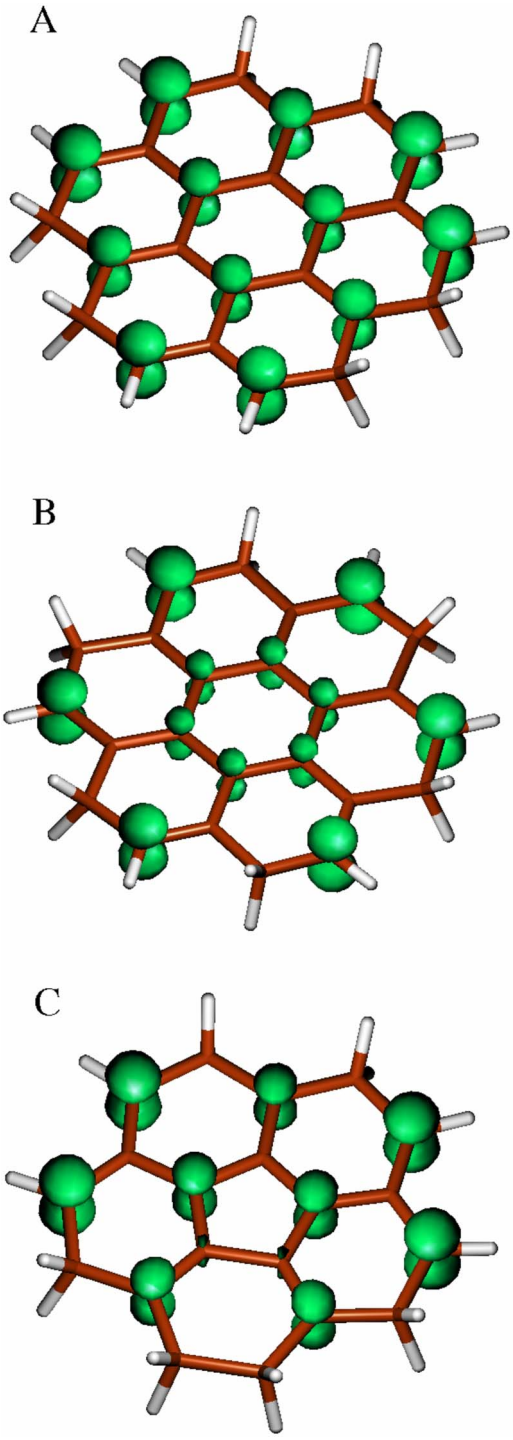

FIG. 3. (Color online) Total spin densities of 1,4,5,8,9,12-hexahydrocoronene and 1,3,5,7,9,11-hexahydrocoronene (both corresponding to septuplets $S=3$) and planar 1,4,5,6,7,10-hexahydrocorannulene ($S=2$ state).

singlet ground state, the spin is equally spread over the two sublattices implying larger electronic repulsions at the central hexagon. The case of 1,4,5,6,7,10-hexahydrocorannulene is even more interesting as, being a frustrated molecule, at least one bond between atoms of the same sublattice should be present. This is clearly visible in Fig. 3 once a sublattice is identified as the sites showing spin density while the rest belong to the other sublattice (colors in Fig. 1 have anticipated this feature). We will show later that the model Hamiltonian calculations for 1,4,5,6,7,10-hexahydrocorannulene show frustration at the same bond than *ab initio* calculations (compare Figs. 3 and 4). Having identified the atoms at each sublattice, it is tempting to use the unbalance in the molecule ($N_A-N_B=4$) to predict the total spin of the ground state using Lieb's formula. The result ($S=2$) is in perfect agreement with numerical results. This is particularly interesting as in principle Lieb's theorem should only work on nonfrustrated systems.

Spin multiplicity of the ground state of a molecule is usually predicted by means of Hund's rule applied to MO energies obtained by an appropriate method. We have checked that the spin of the ground states of the molecules here investigated is consistent with the degeneracy of the HOMO that Hückel's method gives for the skeleton of C atoms having an unsaturated π orbital. This is true not only for 6*H*-coronene but also for 6*H*-corannulene. Although the extended Hückel's method used by *ab initio* codes to initialize the self-consistency process slightly lifts this degeneracy, the HOMO still appears as a narrow bunch containing a number of orbitals compatible with the spin of the ground states of the three planar molecules depicted in Fig. 1. Then, as in Hund's rule, such a distribution of molecular orbitals favors high spin ground states through a winning competition of interaction energy gains against kinetic-energy losses.

IV. MODEL HAMILTONIANS

Let us critically examine the applicability of Lieb's theorem as the predicting tool of the multiplicity of the ground state of hydrogenated PAHs. The underlying Hubbard model ignores that: (i) transfer integrals in any realistic system are not limited to nearest-neighbor sites, (ii) σ orbitals appear around the HOMO-LUMO gap in the same energy interval as π orbitals, and (iii) interaction among electrons is not limited to on-site Coulomb repulsion. In our opinion, the success of a theorem or rule based on the simplest interacting model comes from its actual capability of describing the correct antiferromagnetic spin-spin correlations between nearest π electrons. Strong correlation is the basis for the basic correctness of a simplified image in which up and down spins alternate.[25]

Even if the spin multiplicity of the ground state is predicted either by Hund's rule or Lieb's theorem, a deeper understanding of underlying correlations calls for a complete numerical solution of simple interacting models. We have analyzed both PPP model Hamiltonian[12,13] and the local version of Hubbard Hamiltonian,[26] which actually is a particular case of the former. The PPP Hamiltonian contains a noninteracting part $\hat{H}_0$ and a term that incorporates the electron-electron interactions $\hat{H}_I$,

$$\hat{H} = \hat{H}_0 + \hat{H}_I. \tag{1}$$

The noninteracting term is written as

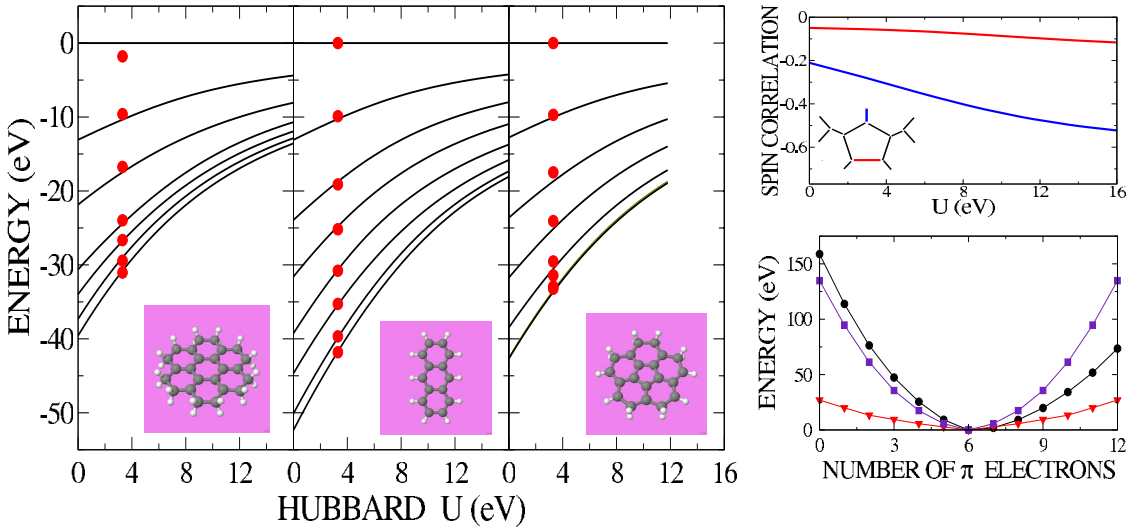

FIG. 4. (Color online) Left: total RB3LYP (circles) and Hubbard model (continuous curves) energies of spin S states versus the on-site Coulomb repulsion U for dodecahydrogenated coronene $C_{24}H_{24}$ (each peripheral carbon atom saturated with an additional hydrogen), anthracene, and 6H-corannulene $C_{20}H_{16}$ [Fig. 1(C)]. The sequences from lowest to highest energy are S=0,1,… for anthracene and $C_{24}H_{24}$ and S=2,1,0,3,4,… for $C_{20}H_{16}$ (in this molecule the Hubbard model gives an almost twofold-degenerate ground state). Energies are referred to the corresponding state of maximum spin except for $C_{24}H_{24}$ that were downward shifted by 1.8 eV to improve the overall fit (the state of S=6 is largely participated by H orbitals turning invalid the Hubbard model). Molecular geometries were only optimized for the ground state and taken unchanged for the calculation of excited spin states. Transfer integral was taken equal to −2.71 eV, and, as the results indicate, U=3.3 eV nicely reproduces the *ab initio* energies. Right up: spin-spin correlations in $C_{20}H_{16}$ calculated by means of the Hubbard model (the skeleton of C atoms is shown as an inset) on blue pair (two atoms placed on the symmetry axis) and red pair (frustrated horizontal bond). Right down: *Ab initio* ground-state energies (circles) of the charged states of a benzene molecule that is not allowed to relax. Energy differences are plotted relative to the neutral case. Results obtained by means of Hubbard (triangles) and Pariser-Parr-Pople (squares) models (Refs. 12 and 13) are also shown.

$$\hat{H}_0 = \epsilon_0 \sum_{i=1,N;\sigma} c_{i\sigma}^{\dagger} c_{i\sigma} + t \sum_{\langle ij\rangle;\sigma} c_{i\sigma}^{\dagger} c_{j\sigma}, \tag{2}$$

where the operator $c_{i\sigma}^{\dagger}$ creates an electron at site i with spin σ, ϵ_0 is the energy of carbon π orbital, and t is the hopping between nearest-neighbor pairs (kinetic energy). N is the number of unsaturated C atoms. The interacting part is in turn given by

$$\hat{H}_I = U \sum_{i=1,N;\sigma} n_{i\uparrow} n_{i\downarrow} + \frac{1}{2} \sum_{i\neq j;\sigma,\sigma'} V_{|i-j|} n_{i\sigma} n_{j\sigma'}, \tag{3}$$

where U is the on-site Coulomb repulsion and $V_{|i-j|}$ is the intersite Coulomb repulsion, while the density operator is

$$n_{i\sigma} = c_{i\sigma}^{\dagger} c_{i\sigma}. \tag{4}$$

This Hamiltonian reduces to the Hubbard model for $V_{|i-j|}=0$.

We start discussing the fitting of spin state energies by means of Hubbard Hamiltonian. Lanczos algorithm in the whole Hilbert occupation space is used to get numerically exact many-body states.[27] Coulomb on-site repulsion has been adjusted to describe spin excitations of some PAHs. Because the interacting model cannot be solved exactly for 6H-coronene (18 orbitals or equivalently sites lead to a Hilbert occupation space of dimension equal to 4^{18} which is beyond actual computational facilities), the case of a coronene molecule with all peripheral C atoms saturated by additional H has been considered. This leaves a molecule with only 12π orbitals, a cluster size that can be easily handled by means of Lanczos algorithm. Also benzene (6 sites), anthracene (14 sites), and 6H-corannulene (14 sites) have been fitted. Calculations were carried out by taking the hopping integral commonly used to describe graphene sheets, t=−2.71 eV, and varying the on-site repulsion U. The results depicted in the left panel of Fig. 4 indicate that spin states of these molecules can be reasonably fitted with U=3.3 eV (benzene, for which the fitting is as good as for anthracene, is not shown for the sake of clarity). Albeit noticeable deviations occur in the three lowest lying states of 6H-corannulene, the state ordering is the correct one. We have checked that the failure to correctly separate the lower excitations of 6H-corannulene is not exclusive of the simplest interacting model: a PPP calculation using Ohno's interpolation scheme[28] shows a similar weakness. Let us remark once more that, despite the rather small U ($U/|t|$=1.27) resulting from the fittings shown in Fig. 4, antiferromagnetic correlations in these molecules, as calculated by means of the interacting model, are significant. Particularly attracting is the case of corannulene for which there is a bond at which the spin-spin correlation is significantly smaller than at other bonds of the molecule (top right panel of Fig. 4). Interestingly enough, placing frustration [two adjacent π orbitals of the same sublattice as shown in Fig. 1(C)] at that bond gives a difference between carbon atoms in the two sublattices of four atoms, which, using Lieb's formula, predicts a ground state of total spin 2, in agreement with our

numerical results. Summarizing, $U=3.3$ eV works satisfactorily describing the spin states of aromatic molecules and, in particular, the multiplicity of the ground state.

The same simple Hubbard model fails, however, in describing the charged states of these systems as shown in the results for benzene (bottom right panel of Fig. 2). Lanczos results for the interacting Hamiltonian are compared with B3LYP results for a charged benzene ideally restricted to a fixed geometric structure. Actual energy differences are much higher than those predicted by the model. Our results do also illustrate the lack of electron-hole symmetry that characterizes any realistic self-consistent field calculation as opposed to Lieb's model. The PPP model with $t=-2.71$ eV and values for the Coulomb repulsion integrals from Ref. 12, although greatly improves the fitting, still gives a symmetric curve by the well-known pairing between occupied and unoccupied molecular orbitals. A full fitting of charge and spin states will surely require including a larger number of parameters.[29,30]

V. CONCLUDING REMARKS

We have proposed a route to produce magnetic organic molecules that consists of hydrogenating PAHs. In the case of alternant PAHs the spin multiplicities of the molecule ground states agree with Lieb's prediction, even though *ab initio* Hamiltonians may significantly differ from Hubbard's model. A probably related result is that *ab initio* energies of the spin states of these molecules can be very satisfactorily fitted by means of the simplest version of the Hubbard model. It seems that the molecule topology is enough support for the main result. Energies of charged molecules, instead, cannot be described by the simple, most popular, interacting models, suggesting a critical examination of their use in, for instance, graphene. Results for total spin densities in molecules having a magnetic ground state clearly show that the spin is localized in only one of the two sublattices. On the other hand, *ab initio* and model Hamiltonian calculations for hydrogenated corannulene place the frustrated bond at the same location. This produces an unbalance in the molecule which, using Lieb's formula, gives $S=2$ for the ground state of the molecule, in agreement with the numerical results. It is also worth noting that in a recent study[31] we have shown that dehydrogenation may also produce magnetic molecules. Although dehydrogenation is a highly unlikely process, dehydrogenated PAHs have been intensively investigated by astrophysicists[32] who believe that they form part of interstellar matter. Although the results presented here are encouraging, there is still a long way to go: finding procedures to synthesize these hydrogenated PAHs and crystallize them into solids that may eventually show magnetic properties.

ACKNOWLEDGMENTS

The authors are grateful to J. Feliu, M. Yus, and A. Guijarro for useful suggestions and remarks. Financial support by the Spanish MCYT (Grants No. FIS200402356, No. MAT2005-07369-C03-01, and No. NAN2004-09183-C10-08) and the Universidad de Alicante is gratefully acknowledged. G.C. is thankful to the Spanish MCYT for a Ramón y Cajal grant.

*jav@icmm.csic.es

[1] J. S. Miller, Inorg. Chem. **39**, 4392 (2000).
[2] R. Jain, K. Kabir, J. B. Gilroy, K. A. R. Mitchell, K.-C. Wong, and R. G. Hicks, Nature (London) **445**, 291 (2007).
[3] A. Rajca, in *Advances in Physical Organic Chemistry 40*, edited by J. Richard (Academic, London, 2005), and references therein.
[4] A. Rajca, J. Wongsriratanakul, and S. Rajca, Science **294**, 1503 (2001).
[5] A. Rajca and S. Rajca, J. Am. Chem. Soc. **118**, 8121 (1996).
[6] L. V. Slipchenko, T. E. Munsch, P. G. Wenthold, and A. I. Krylov, Angew. Chem., Int. Ed. **43**, 742 (2004).
[7] A. I. Krylov, J. Phys. Chem. A **109**, 10638 (2005).
[8] G. P. Pez, A. R. Scott, A. C. Cooper, and H. Cheng, U.S. Patent No. 7,101,530 (September 5, 2006).
[9] G. Zhong, B. Chan, and L. Radom, J. Mol. Struct.: THEOCHEM **811**, 13 (2007).
[10] E. H. Lieb, Phys. Rev. Lett. **62**, 1201 (1989).
[11] A very restricted list of papers reporting on magnetic effects in fullerene and finite graphene systems follows: K. Kusakabe and M. Maruyama, Phys. Rev. B **67**, 092406 (2003); Y.-H. Kim, J. Choi, K. J. Chang, and D. Tomanek, *ibid.* **68**, 125420 (2003); N. Park, M. Yoon, S. Berber, J. Ihm, E. Osawa, and D. Tomanek, Phys. Rev. Lett. **91**, 237204 (2003); De-en Jiang, B. G. Sumpter, and S. Dai, J. Chem. Phys. **127**, 124703 (2007); M. Ezawa, Phys. Rev. B **76**, 245415 (2007); P. Shemella, Y. Zhang, M. Mailman, P. M. Ajayan, and S. K. Nayak, Appl. Phys. Lett. **91**, 042101 (2007); J. Fernández-Rossier and J. J. Palacios, Phys. Rev. Lett. **99**, 177204 (2007); O. Hod, V. Barone, and G. E. Scuseria, Phys. Rev. B **77**, 035411 (2008); K. N. Kudin, ACS Nano **2**, 516 (2008); O. Hod and G. E. Scuseria, *ibid.* **2**, 2243 (2008); E. Rudberg, P. Salek, and Y. Luo, Nano Lett. **7**, 2211 (2007).
[12] R. Pariser and R. G. Parr, J. Chem. Phys. **21**, 466 (1953).
[13] J. A. Pople, Trans. Faraday Soc. **49**, 1365 (1953).
[14] J. Andzelm, M. Klobukowski, E. Radzio-Andzelm, Y. Sakai, and H. Tatewaki, in *Gaussian Basis Sets for Molecular Calculations*, edited by S. Huzinaga (Elsevier, Amsterdam, 1984).
[15] T. H. Dunning, Jr., J. Chem. Phys. **90**, 1007 (1989).
[16] A. D. Becke, J. Chem. Phys. **98**, 5648 (1993).
[17] C. Lee, W. Yang, and R. G. Parr, Phys. Rev. B **37**, 785 (1988).
[18] R. Colle and O. Salvetti, Theor. Chim. Acta **37**, 329 (1975).
[19] Remember that unrestricted-Hartree-Fock calculations do not provide wave functions with a defined total spin (only one component is a good quantum number).
[20] B. R. Brooks and H. F. Schaefer III, J. Chem. Phys. **70**, 5092 (1979).
[21] M. W. Schmidt and M. S. Gordon, Annu. Rev. Phys. Chem. **49**, 233 (1998).
[22] B. Roos, Adv. Chem. Phys. **69**, 399 (1987).
[23] M. W. Schmidt, K. K. Baldridge, J. A. Boatz, S. T. Elbert, M. S.

Gordon, J. H. Jensen, S. Koseki, N. Matsunaga, K. A. Nguyen, S. J. Su, T. L. Windus, M. Dupuis, and J. A. Montgomery, J. Comput. Chem. **14**, 1347 (1993).

[24] C. Melero, R. P. Herrera, A. Guijarro, and M. Yus, Chem.-Eur. J. **13**, 10096 (2007).

[25] Let us mention two recently published examples. Antiferromagnetic correlations have been found both at the edges of graphene nanoribbons [see, Y.-W. Son, M. L. Cohen, and S. G. Louie, Nature (London) **444**, 347 (2006)] and at the (110) surface of diamond [see F. Yndurain, Phys. Rev. B **75**, 195443 (2007)]. Some of the papers listed in Ref. 11 include further examples.

[26] J. Hubbard, Proc. R. Soc. London, Ser. A **276**, 238 (1963).

[27] We use a straightforward Lanczos transformation starting from a random ground state candidate to generate a small Hamiltonian matrix that can be diagonalized to get a better approximation for the ground state. This process is iterated until convergence is reached [see G. Chiappe, E. Louis, J. Galán, F. Guinea, and J. A. Vergés, Phys. Rev. B **48**, 16539 (1993) for details].

[28] K. Ohno, Theor. Chim. Acta **2**, 219 (1964).

[29] R. Oszwaldowski, H. Vázquez, P. Pou, J. Ortega, R. Pérez, and F. Flores, J. Phys.: Condens. Matter **15**, S2665 (2003).

[30] G. Chiappe, E. Louis, E. San Fabián, and J. A. Vergés, Phys. Rev. B **75**, 195104 (2007).

[31] J. A. Vergés, E. San Fabián, L. Pastor-Abia, G. Chiappe, and E. Louis, Phys. Status Solidi (b) (to be published).

[32] V. Le Page, T. P. Snow, and V. M. Bierbaum, Astrophys. J. **584**, 316 (2003).